Earth Planets Space, **65**, 385–396, 2013

On the coupling of fast and shear Alfvén wave modes by the ionospheric Hall conductance

C. L. Waters[1], R. L. Lysak[2], and M. D. Sciffer[1]

[1]*School of Mathematical and Physical Sciences, University of Newcastle, New South Wales, Australia*
[2]*School of Physics and Astronomy, University of Minnesota, Minneapolis, Minnesota, U.S.A.*

(Received April 3, 2012; Revised July 24, 2012; Accepted August 24, 2012; Online published June 10, 2013)

There are two low frequency, magnetised, cold plasma wave modes that propagate through the Earth's magnetosphere. These are the compressional (fast) and the shear Alfvén modes. The fast mode distributes energy throughout the magnetosphere with the ability to propagate across the magnetic field. Previous studies of coupling between these two modes have often focussed on conditions necessary for mode coupling to occur in the magnetosphere. However, Kato and Tamao (1956) predicted mode coupling would occur for non-zero Hall currents. Recently, the importance of the Hall conductance in the ionosphere for low frequency wave propagation has been studied using one dimensional (1-D) models. In this paper we describe effects of the ionosphere Hall conductance on field line resonance and higher frequency, 0.1–5 Hz waves associated with the Ionospheric Alfvén Resonator (IAR). The Hall conductance reduces the damping time of field line resonances and Joule dissipation into the ionosphere. The Hall conductance also couples shear Alfvén waves trapped in the IAR to fast mode waves that propagate across the ambient magnetic field in an ionospheric waveguide. This coupling leads to the production of low frequency magnetic fields on the ground that can be observed by magnetometers.
Key words: ULF waves, Hall current, ionosphere.

1. Introduction

Near-Earth space is a dynamic region energised by solar processes. The solar wind and magnetosphere of Earth interact to produce perturbations in the magnetised plasma with a wide range of spatial and temporal scales. The ULF band (0.001–5 Hz) encompasses the continuous (Pc1–5) and irregular (Pi1 and 2) type perturbations as classified by Jacobs *et al*. (1964). In the magnetosphere, these waves represent a range in wavelength scale of a factor of ≈1000. This early classification was based on the appearance of time series and spectral representations, with little information available on generation mechanisms.

Ground based sensors, such as sensitive magnetometers, detect ULF wave signatures and these observations are used to deduce generation and propagation mechanisms which in turn provide information on the structure and dynamics of the magnetosphere. An understanding of ULF wave propagation through the ionosphere-atmosphere system is important for using ULF wave properties to remote sense the magnetosphere. Present understanding of generation and propagation properties of the more continuous pulsations suggests a broad grouping of two, the Pc1–2 and Pc3–5 bands. In this paper we highlight the effects of ionospheric Hall conductance on ULF wave interaction with the magnetosphere-ionosphere-atmosphere-ground system, an important factor recognised by Kato and Tamao (1956). Sections 1–4 focus on pulsations in the Pc3–5 range and demonstrate ULF wave mode coupling arising from the anisotropic ionosphere even for a zero azimuthal wave number. Sections 5–8 focus in the higher frequency Pc1–2 band and the effects of Hall conductance on the ionospheric Alfvén resonator.

Early studies of ULF wave transition from the magnetised plasma environment of near Earth space to the atmosphere reported a 'shielding' or 'screening' effect (e.g. Ashour and Price, 1948). Nishida (1964) summarised understanding at the time for frequencies, $\omega < 0.1$ rad/s. For the appropriate wave mode, the ionosphere modification was understood as a rotation in the direction of the wave magnetic field (polarisation azimuth) by 90° plus an 'appreciable' decrease in magnitude at the ground. A common simplification in modeling the situation was to assume a vertical background magnetic field, $\mathbf{B}_0$. Francis and Karplus (1960) also assumed vertical wave propagation.

Dungey (1963) developed analytic solutions by dividing the problem into toroidal (divergence free) and poloidal (curl free) magnetic field components, linking these with the shear and fast Alfvén, ideal magnetohydrodynamic (MHD) wave modes that exist in the cold, magnetised plasma of the magnetosphere (Stix, 1962; Alfvén and Fälthammar, 1963). This appears to have been a common approach at the time, as Kato and Tamao (1956) contains a similar analysis while referring to the contemporary literature that used a similar mathematical development. This approach was also used in subsequent treatments (e.g. Hughes, 1974) and in more recent studies of magnetosphere-ionosphere coupling (e.g. Yoshikawa and

doi:10.5047/eps.2012.08.002

Itonaga, 2000). The assumption of ideal MHD physics for the magnetosphere and a vertical $\mathbf{B}_0$ simplifies the problem since for these conditions, the shear Alfvén and fast mode electric fields are orthogonal, as discussed by Sciffer *et al.* (2004).

Kato and Tamao (1956) examined the effect of the ionosphere Hall conductivity on ULF waves. They pointed out that 'the poloidal and the toroidal type fields will couple with each other'. While Tamao (1965) discussed ULF wave mode coupling in the magnetosphere, in this paper we focus on the insight of Kato and Tamao (1956) who, ten years earlier had recognised that the two cold plasma Alfvén waves would couple through the Hall conductance of the ionosphere. Until recently, subsequent studies neglected ionospheric Hall current effects on ULF waves.

The importance of the Hall conductance for ULF waves interacting with the ionosphere has recently been revived. An inductive shielding effect (ISE) was discussed by Yoshikawa *et al.* (2002) for the case where $\mathbf{B}_0$ is vertical. The ISE may be understood in terms of the properties of the ULF wave electric field, $\mathbf{E}$. If $\nabla \times \mathbf{E}$ is significant, then Faraday's inductive term causes a reduction in amplitude of the waves seen on the ground compared with those in the magnetosphere (Yoshikawa and Itonaga, 1996, 2000; Sciffer *et al.*, 2004). Alternatively, assuming constant Alfvén speed above the ionosphere, Pilipenko *et al.* (2000) interpreted the inductive process as a partial conversion of the incident shear Alfvén wave into an ionospheric surface wave.

The ionosphere presents a partially conducting interface between the magnetosphere and the atmosphere. In the electrostatic limit, $\nabla \times \mathbf{E} = 0$ in the ionosphere and Scholer (1970) showed that the reflection coefficient for a shear Alfvén wave is

$$\Gamma_{AA} = \frac{\Sigma_A - \Sigma_P}{\Sigma_A + \Sigma_P} \tag{1}$$

where Σ_A is the Alfvén wave conductance and Σ_P is the height integrated Pedersen conductivity (Pedersen conductance). This assumes that $\mathbf{B}_0$ is vertical, only the shear Alfén wave is present in the system and Hall current effects are negligible.

In reality, fast mode oscillations are also present and Hall currents are significant. If we have a shear Alfvén mode incident from the magnetosphere, the ionosphere Pedersen current closes the field aligned current (for vertical $\mathbf{B}_0$) while the eddy current of the inductive response is the ionosphere Hall current which then generates a fast mode in the ionosphere that may be detected in the magnetosphere and at the ground (Tamao, 1965). This introduces wave mode conversion coefficients between the shear and fast Alfvén modes, expanding the single reflection coefficient of Eq. (1) into a 2×2 reflection and wave mode conversion matrix.

A number of analytical studies have provided reflection and mode conversion coefficients and Poynting flux details (e.g. Sorokin, 1986; Alperovich and Fedorov, 1992; Yoshikawa and Itonaga, 1996). All these models assumed a vertical $\mathbf{B}_0$. The expressions for the reflection and mode conversion coefficients allowing for both fast and shear incident Alfvén wave modes, the inductive shielding effect and oblique $\mathbf{B}_0$ were developed by Sciffer and Waters (2002) with typographic errors corrected in Sciffer *et al.* (2004). The 2×2 reflection and mode conversion matrix specifies the interaction of the combined ionosphere-atmosphere-ground system with both the fast and shear Alfvén modes.

The recently revived interest in Hall current effects on the transition of ULF waves from the magnetosphere through to the ground have been investigated using one-dimensional model approximations. Both simplified analytic approximations and more realistic numerical calculations have revealed the basic effects of the inductive process involved with the Hall conductance. Initial experimental verification in the Pc3 band has shown the expected amplitude change with ionospheric conductance (e.g. Obana *et al.*, 2005). However, higher dimensional models are required to more realistically simulate spatial structures that are inconsistent with the assumed $e^{i\mathbf{k}\cdot\mathbf{r}}$ spatial variations used in 1-D models. An important example is the spatial structure of ULF wave fields across a field line resonance, which also involves a varying mix of fast and shear Alfvén modes and this case is discussed below.

2. ULF Wave Model

A detailed description of a time dependent, 2-D ULF wave model with $e^{im\phi}$ variation in the third dimension, using distorted dipole coordinates was given by Lysak (2004) and Waters and Sciffer (2008). A first approximation to the geomagnetic field in the inner magnetosphere ($\leq 5\ R_E$) is a dipole geometry. However, spherical geometry is more suitable for the ionosphere. In order to simplify the ionosphere boundary conditions yet model ULF waves in a dipole geometry, a distorted dipole coordinate system was developed by Lysak (2004). Define a (contravariant) coordinate set (u^1, u^2, u^3) that is a function of the spherical coordinates, (R, θ, ϕ) and then define two sets of basis vectors, one tangential to the geomagnetic field with the other set orthogonal to the ionosphere current sheet. If $\mathbf{R}$ is the position vector in spherical coordinates then the covariant (tangential) basis vectors, $\mathbf{v_i}$, are defined by

$$\mathbf{v_i} = \frac{\partial \mathbf{R}}{\partial u^i} = \partial_i \mathbf{R} \tag{2}$$

while the contravariant (cotangent, reciprocal, dual, normal or gradient) basis vectors, $\mathbf{v^i}$, are

$$\mathbf{v^i} = \nabla u^i. \tag{3}$$

These basis vectors are related such that $\mathbf{v}^i \cdot \mathbf{v}_j = \delta^i_j$. The Jacobian of the transformation from (u_1, u_2, u_3) to (R, θ, ϕ) is

$$J = \frac{\partial(R, \theta, \phi)}{\partial(u_1, u_2, u_3)} = \mathbf{v_1} \cdot (\mathbf{v_2} \times \mathbf{v_3}). \tag{4}$$

We use the coordinate system (Lysak, 2004)

$$u^1 = -\frac{R_I}{R} \sin^2 \theta \tag{5}$$

$$u^2 = \phi \tag{6}$$

$$u^3 = -\frac{R_I^2 \cos\theta}{R^2 \cos\theta_0} \tag{7}$$

where R_I is the radius of the ionosphere and R is the radial distance from the centre of Earth to the particular point

in space, a (R, θ) coordinate for a 2-D description. The model assumes an azimuthal dependence of all electric and magnetic fields of the form $e^{im\phi}$ where m is the azimuthal wave number (Olson and Rostoker, 1978). All distances are scaled in units of R_E (the Earth's radius), θ is the colatitude while θ_0 is the colatitude at the surface of Earth in the northern hemisphere after tracing along the magnetic field from a point (R, θ). Therefore, θ_0 is given by $\cos\theta_0 = \sqrt{1 - R_I/L} = \sqrt{1 + u^1}$.

The Maxwell equations may be reformulated using the covariant and contravariant basis vectors (D'haeseleer *et al.*, 1991). In the magnetosphere, $\mathbf{v}_3$ is tangential to the geomagnetic field so the ULF electric field component, $\mathbf{E}_3 = 0$ for the ideal MHD approximation. The equations to be solved are

$$\frac{\partial E^1}{\partial t} = \frac{V^2}{J}\,(imb_3 - \partial_3 b_2) \tag{8}$$

$$\frac{\partial E^2}{\partial t} = \frac{V^2}{J}\,(\partial_3 b_1 - \partial_1 b_3) \tag{9}$$

$$\frac{\partial b^1}{\partial t} = \frac{1}{J}\,(\partial_3 E_2) \tag{10}$$

$$\frac{\partial b^2}{\partial t} = -\frac{1}{J}\,(\partial_3 E_1) \tag{11}$$

$$\frac{\partial b^3}{\partial t} = \frac{1}{J}\,(imE_1 - \partial_1 E_2) \tag{12}$$

where $V^2 = \frac{1}{\mu_0 \epsilon_\perp}$. Equations (8) to (12) were solved over a Yee, staggered grid with a leapfrog technique for the time iteration (Taflove and Hagness, 2005).

On the inner L shell boundary ($L = 1.2$), E_2 and b_1 were set to zero. Using (9), this also sets $\partial_1 b_3 = 0$ so the inner boundary is perfectly reflecting. The outer boundary was driven by a sinusoidal time varying function with a gaussian spatial dependence for b_3 on the outer field line at 10 R_E. Specifically, the driver function was of the form

$$b_3(u_3, t) = \Gamma(u_3)\ \sin\left[2\pi f_c\left(t - \frac{2}{\delta f_c}\right)\right] e^{-[(t-\frac{2}{\delta f_c})\delta f_c]^2} \tag{13}$$

where Γ is a gaussian function of distance along the outer field line, f_c is the carrier frequency and δf_c the bandwidth of the driver. For this paper, $f_c = 5$ mHz with $\delta f_c = 4$ mHz.

The ionosphere current density is described by $\Sigma \cdot \mathbf{E}$. The horizontal ionosphere electric field components, E_1 and E_2, and the radial magnetic field component, b^3 are continuous across the ionosphere current sheet. The ionospheric boundary is given by (Hughes, 1974; Yoshikawa and Itonaga, 2000; Sciffer and Waters, 2002)

$$\mu_0 \Sigma \cdot \mathbf{E} = \hat{\mathbf{r}} \times \Delta\mathbf{b} \tag{14}$$

where Σ is the height integrated conductivity tensor and $\Delta\mathbf{b}$ is the discontunity in the ULF magnetic field across the current sheet. For an oblique geomagnetic field, the conductivity tensor is (Lysak, 2004)

$$\Sigma = \begin{bmatrix} \dfrac{\Sigma_0 \Sigma_P}{\Sigma_{zz}} & -\dfrac{\Sigma_0 \Sigma_H \cos\alpha}{\Sigma_{ZZ}} \\ \dfrac{\Sigma_0 \Sigma_H \cos\alpha}{\Sigma_{ZZ}} & \Sigma_P + \dfrac{\Sigma_H^2 \sin^2\alpha}{\Sigma_{ZZ}} \end{bmatrix} \tag{15}$$

where Σ_P, Σ_H and Σ_0 are the height integrated Pedersen, Hall and direct conductivities respectively. The direct conductivity relates the geomagnetic field aligned electric fields and currents. The angle between the geomagnetic field and the radial direction, α is given by

$$\cos\alpha = -2\cos\theta/\sqrt{1 + 3\cos^2\theta_0} \tag{16}$$

while

$$\Sigma_{ZZ} = \Sigma_0 \cos^2\alpha + \Sigma_P \sin^2\alpha. \tag{17}$$

The atmosphere is described by $\nabla \cdot \mathbf{b} = \nabla \times \mathbf{b} = 0$ so the ULF magnetic field may be expressed in terms of a scalar potential, Ψ where $\mathbf{b} = -\nabla\Psi$ and $\nabla^2\Psi = 0$. The Laplace equation in the atmosphere is solved using spherical harmonic functions to obtain the magnetic field below the current sheet. These are spherical harmonic eigenfunctions over the colatitude range corresponding to $L = 1.2$ and $L = 10$. For ULF waves, the ground is a good conductor so the radial component of the wave magnetic field at the ground is set to zero (i.e. $b_R = \frac{\partial\Psi}{\partial R} = 0$ at $R = R_E$). At the ionosphere current sheet, continuity in the radial magnetic field sets $b_R = \frac{\partial\Psi}{\partial R} = h_R b^3$ where h_R is the radial scale factor on the spherical harmonics at the ionosphere.

In the magnetosphere, the Alfvén speed, $V_A = B_0/\sqrt{\mu_0\rho}$ varies with position. A power dependence for the plasma mass density was used

$$\rho(R) = \rho_{eq}\left(\frac{L}{R}\right)^6 + \rho_i e^{-(R-R_E)/\lambda_i}. \tag{18}$$

where R is the distance from Earth centre in R_E and ρ_{eq} is the equatorial plasma mass density which is a function of the McIlwain L number. The second term represents the increased mass loading near the ionosphere. The ρ_i is the ionosphere mass density while λ_i is the scale height of the mass loading. For this paper $\lambda_i = 0.04$ R_E (250 km) and $\rho_i = 10^7$ kg/R_E^3.

3. Wave Mode Coupling by the Ionosphere

An inspection of Eqs. (8) to (12) shows that when the azimuthal wavenumber, $m = 0$ then Eqs. (9), (10) and (12) describe the fast mode while Eqs. (8) and (11) are the shear Alfvén mode. When the model is driven by b_3 with $m = 0$ then only the dipole ULF components of b_ν, b_μ and E_ϕ are non-zero. However, this only occurs if the ionosphere Hall conductance is also zero. Figure 1 shows shaded 2-D, time snapshots of the ULF field components after 800 s when $m = 0$ and the Hall conductance, $\Sigma_H = 10$ S.

The time development shows fast mode energy propagates inward with signal on b_μ, b_ν and E_ϕ. After the travel time to the ionosphere has elapsed (a minute or so), signal appears on the shear Alfvén components, b_ϕ and E_ν. The E_ν component is shown with a well formed field line resonance at 6 R_E. The inbound fast mode interacts with the anisotropic ionosphere, partially converts to the shear Afvén mode and excites field line resonances at the appropriate latitudes. This process shows the importance of realistic inner boundary conditions to describe ULF wave mode coupling in the magnetosphere.

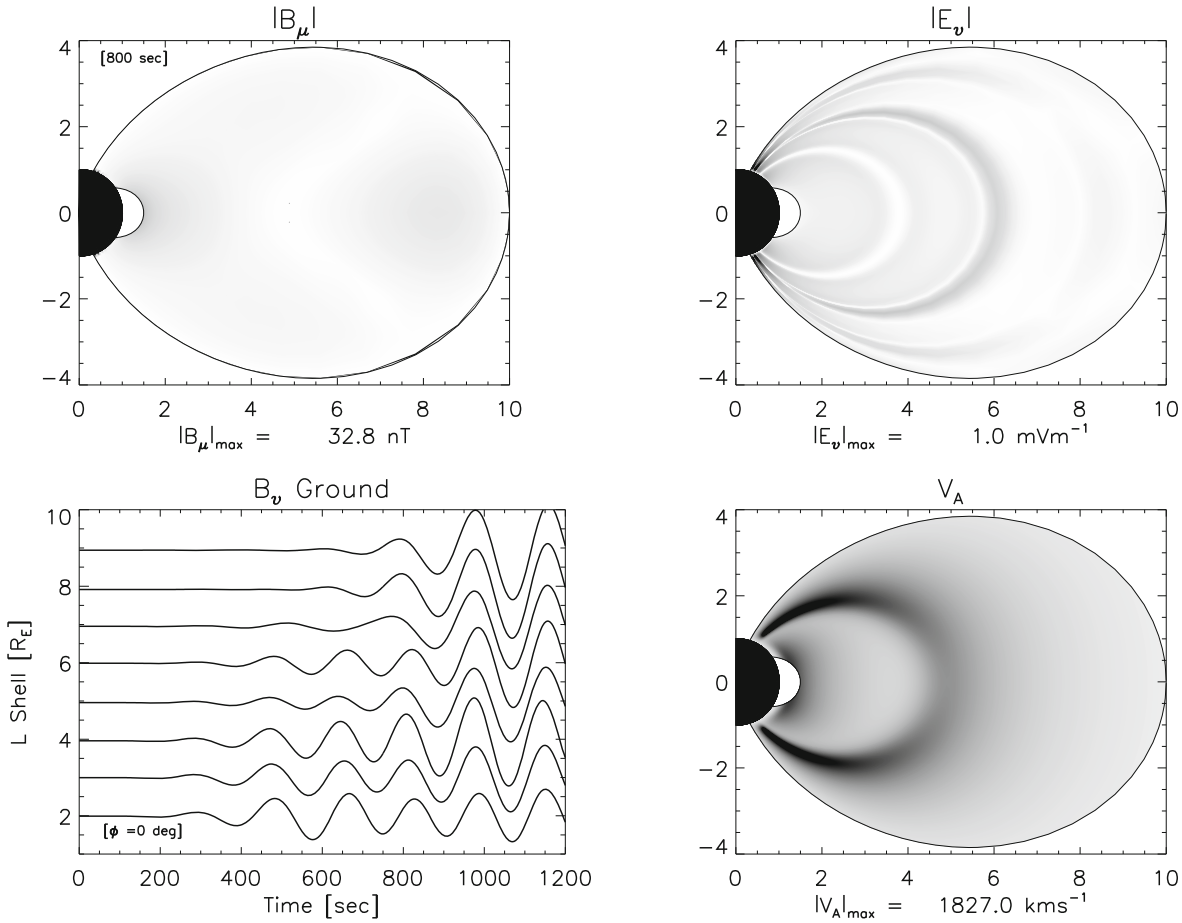

Fig. 1. ULF field components for $m = 0$, $\Sigma_P = 5$ S and $\Sigma_H = 10$ S. Snapshots at $t = 800$ s of the fast mode magnetic field (top, left) and shear mode electric field (top, right) show fast to shear mode coupling for $m = 0$. The north-south ground magnetic fields over $t = 0$–1200 s are shown at bottom, left. The spatial variation of the Alfvén speed used in the model is shown at bottom, right.

4. Hall Conductance and Wave Energy in the Ionosphere

Conservation of energy for electromagnetic waves is described by the Poynting theorem (e.g. Jackson, 1999)

$$\nabla \cdot (\mathbf{E} \times \mathbf{B}) = -\left(\epsilon_0 \mathbf{E} \cdot \frac{\partial \mathbf{E}}{\partial t} + \frac{\mathbf{B}}{\mu_0} \cdot \frac{\partial \mathbf{B}}{\partial t}\right) - \mathbf{J} \cdot \mathbf{E} \quad (19)$$

where $\mathbf{J} \cdot \mathbf{E}$ is the Joule heating term. If $m = 0$ and also $\Sigma_H = 0$ then Joule dissipation of ULF energy in the ionosphere only occurs through the Pedersen conductance as $\Sigma_P E^2$.

Figure 2(a) shows the time development of the Joule heating in the northern ionosphere for Pc5 (5 mHz) excitation on b_μ in the 2-D model. For this case $m = 0$ while $\Sigma_P = 5$ S and $\Sigma_H = 10$ S in the spatially uniform ionospheres. The 5 mHz, incoming fast mode partially converts to a shear Alfvén fundamental resonance near 6 R_E. Most of the $\mathbf{J} \cdot \mathbf{E}$ energy in the ionosphere is driven by the fast mode. There is mode conversion near 6 R_E showing that the Hall current in the ionosphere provides a pathway for energy to flow into the resonance even for $m = 0$.

Figure 2(b) shows the time development of $\mathbf{J} \cdot \mathbf{E}$ in the ionosphere when the azimuthal wave variation has $m = 2$. Fast to shear Alfvén wave mode coupling now occurs in both the magnetosphere and ionosphere and the FLR dominates the energy dynamics. As time progresses, the resonance narrows in latitude in addition to developing a distinct poleward motion. The specific details of these features depends on the ionosphere conductance, m number and the properties of the radial gradient in the Alfvén speed in the magnetosphere.

The effects of Hall conductance on the Joule heating over the spatial structure of a field line resonance are shown in Fig. 3. The solid line in Fig. 3(a) shows the magnitude of $\mathbf{J} \cdot \mathbf{E}$ when $\Sigma_H = 0$ and $m = 0$. For this case, the Joule dissipation is just $\Sigma_P E^2$, and decreases with decreasing radial distance as the wave amplitude reduces from energy loss as the wave propagates inward. The dotted and dashed lines show the effect of increasing Σ_H. For non-zero Σ_H, Joule dissipation is reduced overall and is further reduced at field line resonance locations.

The effects of Hall conductance on the Joule heating for $m = 2$ are shown in Fig. 3(b). This appears to be the type of situation encountered in experimental data where Joule dissipation in the ionosphere is increased at FLR locations (e.g. Greenwald and Walker, 1980). The peak out near 8.5 R_E corresponds with the third FLR harmonic and the Joule heating is reduced for increased Σ_H, as indicated in Fig. 3(a). For the fundamental FLR at $L = 6$, the amount of Joule heating depends on both the decrease indicated in Fig. 3(a) and the relative amount of energy that propagated past the $L = 8.5$, third harmonic interaction.

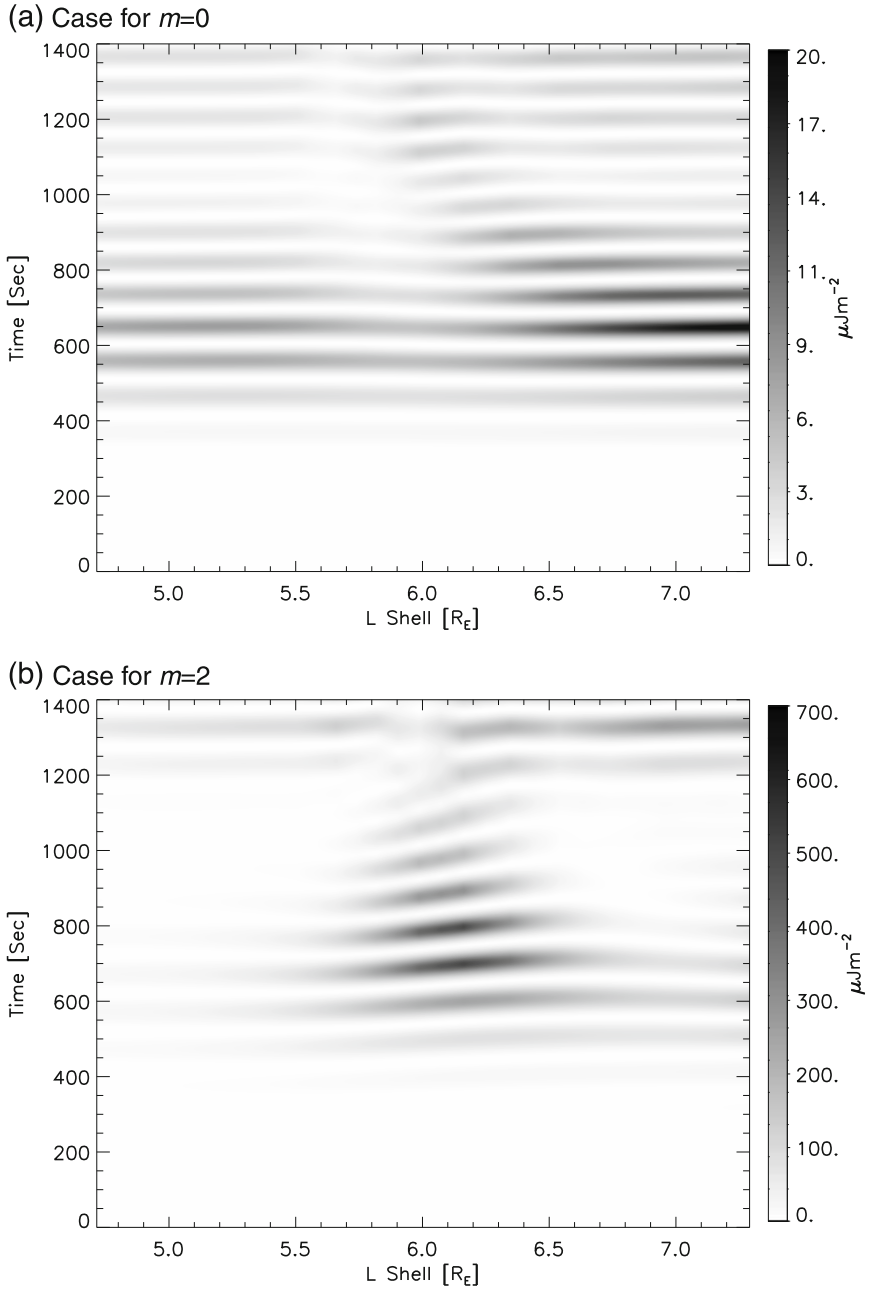

Fig. 2. Ionosphere Joule heating as functions of time and mapped radial distance with $\Sigma_P = 5$ S and $\Sigma_H = 10$ S.

One consequence of lower energy loss to the ionosphere from increased Σ_H at resonance is illustrated in Fig. 4. The spectral amplitude of the equatorial E_v component located at the fundamental FLR ($L \approx 6\ R_E$), for the $m = 2$ case was calculated. The model driver used Eq. (13) with $f_c = 5$ mHz, $\delta f_c = 4$ mHz. The driver term was turned off after 900 s. The amplitude of the 5 mHz signal was calculated using a Fast Fourier Transform (FFT) with a window length of 1000 s. Each FFT was overlapped by 95%.

For the zero Hall conductance case (solid line) the maximum amplitude occurs when the driver signal is turned off. The amplitude decreases to $e^{-1} = 1/2.7183$ of the original amplitude, shown by the dash-dotted, horizontal line. For $\Sigma_H = 0$, the exponential decay time is ≈ 700 s. However, for $\Sigma_H = 5$ S the decay time increases to ≈ 900 s and for $\Sigma_H = 10$ S, the decay time increases further to ≈ 1400 s. These are very similar to FLR ringtime values obtained from an analysis of AMPTE/CCE spacecraft data by Anderson and Engebretson (1989). Increasing the Hall conductance allows the energy to oscillate through the inductive process rather than dissipate as Joule heating, increasing the 'ringtime' of field line resonances. Even though the Hall conductance does not contribute directly to Ohmic loss, a non-zero Hall conductance affects the damping time of FLR's by reducing the amount of energy lost each cycle.

5. Pc1 Pulsations and the Ionospheric Alfvén Resonator (IAR)

It has long been known from ground observations that Pc1 waves are common in the ionosphere (e.g., Jacobs and Watanabe, 1962; Manchester, 1968; Fraser, 1975; Hansen *et al.*, 1992; Popecki *et al.*, 1993; Neudegg *et al.*, 1995).

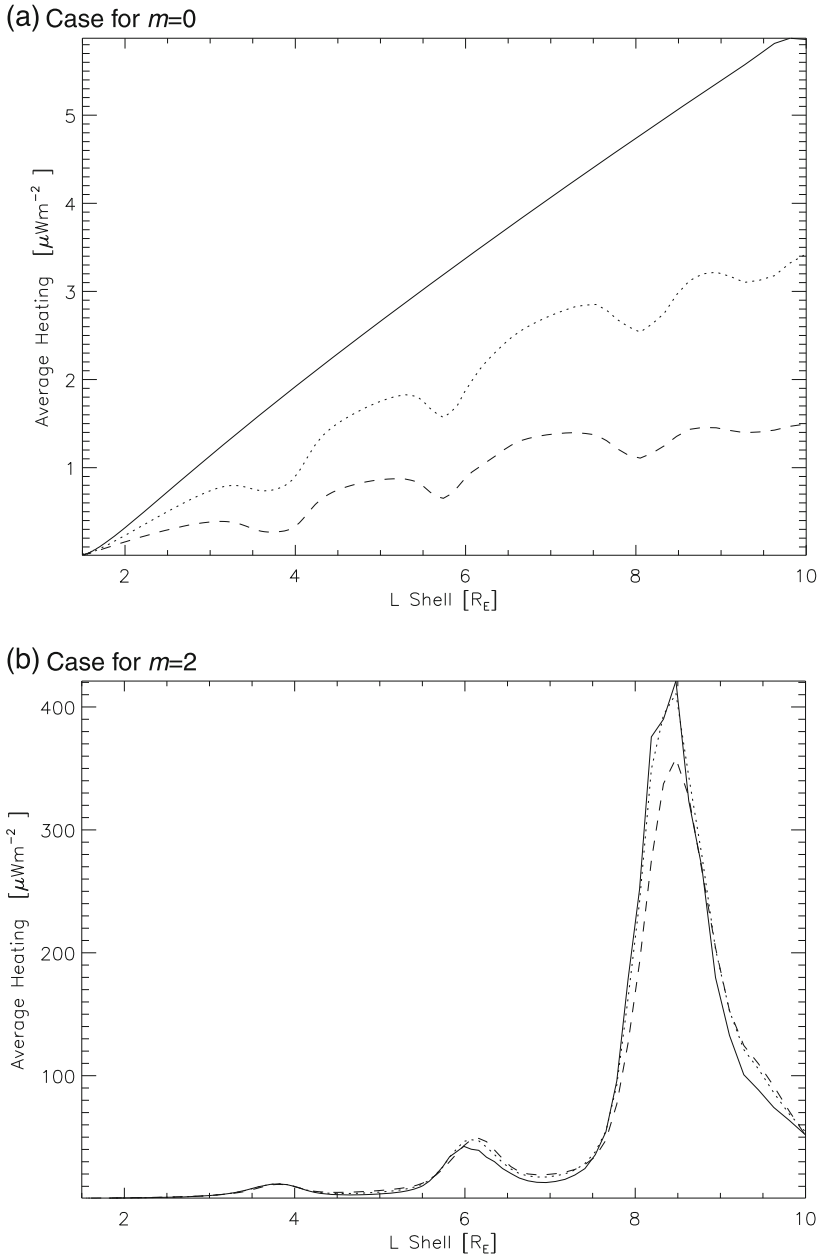

Fig. 3. Joule heating in the ionosphere for $\Sigma_P = 5$ S and $\Sigma_H = 0$ S (solid), $\Sigma_H = 5$ S (dotted) and $\Sigma_H = 10$ S (dashed).

Simultaneous observations of Pc1 waves by ground magnetometers and the Viking satellite were reported by Arnoldy *et al.* (1988, 1996) and Potemra *et al.* (1992). Temerin *et al.* (1981) noted that S3-3 satellite observations of large quasi-static electric fields are consistent with being electrostatic structures at high altitudes. At altitudes below 5000 km, however, the observed electric fields were more consistent with being large amplitude Alfvén waves.

Dynamics Explorer observations (Gurnett *et al.*, 1984) have also indicated that low frequency electric and magnetic field observations are consistent with an Alfvén wave interpretation. Similar results have been obtained by the ICB-1300 satellite (Chmyrev *et al.*, 1985), Aureol-3 (Berthelier *et al.*, 1989), Magsat (Iyemori and Hayashi, 1989), HILAT (Knudsen *et al.*, 1990, 1992), Freja (Grzesiak, 2000), FAST (Chaston *et al.*, 2002b), Akebono (Hirano *et al.*, 2005) and sounding rockets (Boehm *et al.*, 1990). Viking observations have shown that the peak power of electric and magnetic fluctuations occur in this frequency range (Block and Fälthammar, 1990; Erlandson *et al.*, 1990; Marklund *et al.*, 1990). Volwerk *et al.* (1996) reported a small compressional component in association with the Alfvén wave, consistent with a coupling between these two wave modes.

Recent observations have verified that waves in this frequency range are common, not only at auroral latitudes but also at lower latitudes. Belyaev *et al.* (1999) observed the spectral signatures of the resonator from ground magnetometer observations and have shown that the frequency structure was consistent with the resonator, and varied during the day consistent with ionospheric density measurements from the EISCAT radar. Grzesiak (2000) showed using Freja data that the phase relationships predicted by the theory of the resonator (Lysak, 1991) were consistent with the data. Recent observations from Akebono (Hirano *et al.*,

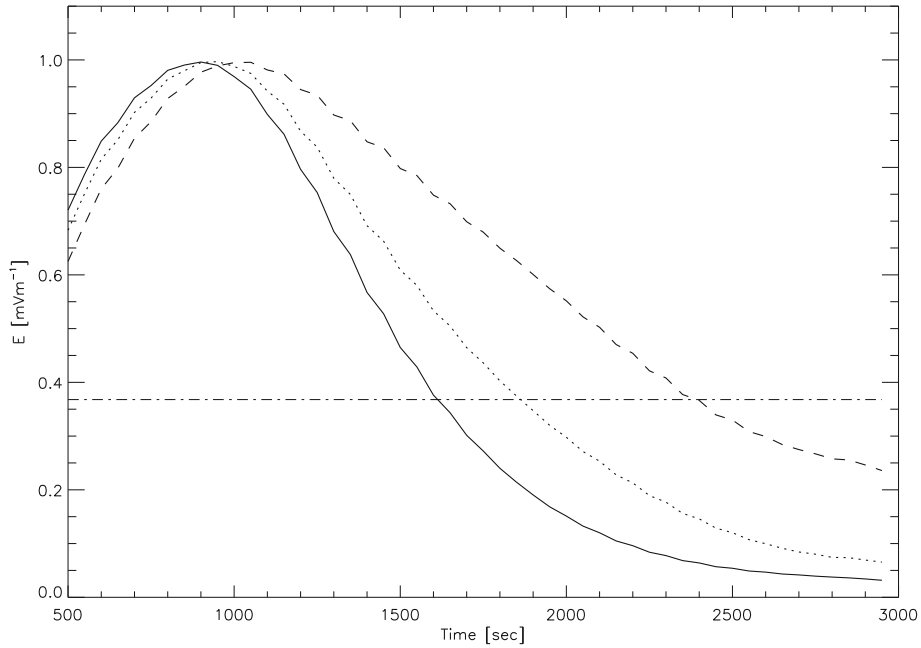

Fig. 4. Amplitude of the 5 mHz, E_v ULF wave component for $m = 2$, $\Sigma_P = 5$ S and $\Sigma_H = 0$ S (Solid), 5 S (dotted) and 10 S (dashed), in the equatorial plane at the fundamental FLR location ($L \approx 6\ R_E$). The dotted-dashed line shows the exponential decay amplitude level.

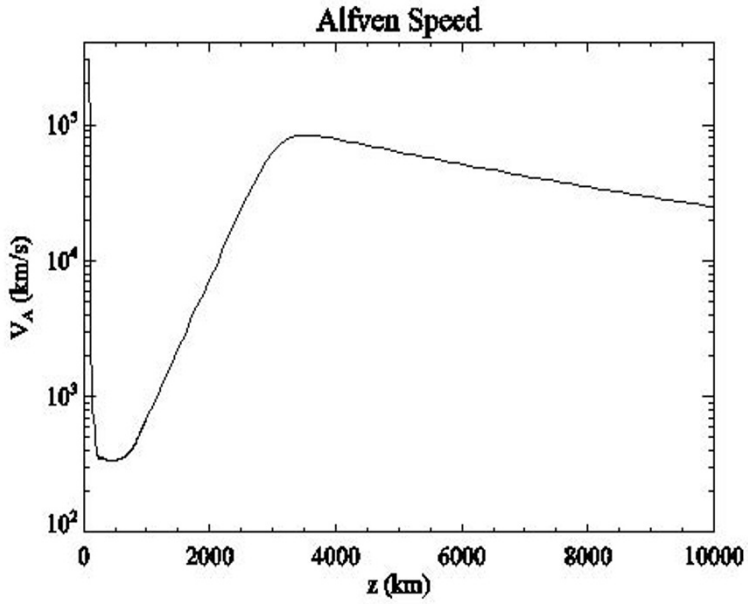

Fig. 5. Alfvén speed near the ionosphere showing the ionosphere Alfvén resonator caivty in V_A.

2005) and from a sounding rocket (Tanaka *et al.*, 2005) have shown IAR signatures in the cusp and the related modulation of precipitating electrons.

Explanations for these observations have focused on the properties of the MHD wave modes and Alfvén speed in the topside ionosphere. The strong inhomogeneities in plasma density and thus Alfvén speed in the ionosphere and adjacent regions can trap waves in the upper end of the ULF range (Pc1). Since the mass density decreases exponentially with increasing altitude in the topside ionosphere while the magnetic field decreases less rapidly, the Alfvén speed increases rapidly, reaching a peak at an altitude of about 1 R_E that can be comparable to the speed of light. The behavior in the wave speed up to 10,000 km altitude for typical parameters based on the MSIS atmosphere and International Reference Ionosphere (IRI) models is shown in Fig. 5. The deep minimum in the wave speed in the ionosphere forms a resonant cavity, termed the ionospheric Alfvén resonator (IAR) by Polyakov and Rapoport (1981) and studied extensively by Trakhtengertz and Feldstein (1984, 1991) and Lysak (1986, 1991, 1993). This cavity has resonant frequencies in the range of 0.1–1.0 Hz.

6. Simplified Model for the Shear Alfvén Mode in the IAR

Models for these observations initially treated the shear and fast Alfvén modes separately. Consider the shear mode wave equation in an inhomogeneous medium. If we consider a plane wave variation in the perpendicular direction $e^{ik_\perp x}$ and oscillations at a frequency ω, then an ideal, shear Alfvén wave will consist of E_x and b_y components, where $\mathbf{z}$ is the vertical direction, parallel or anti-parallel to the magnetic field in the southern and northern ionospheres, respectively. In this case, the MHD equations can be combined into a wave equation,

$$\frac{\partial E_x}{\partial z^2} + \frac{\omega^2}{V_A^2(z)} E_x = 0 \tag{20}$$

which has the form of a Schrödinger equation, where the effective potential is related to the Alfvén speed.

The next step is to choose a profile for V_A along the field line such as that shown in Fig. 5. Some authors (e.g., Trakhtengertz and Feldstein, 1984; Fedorov *et al*., 2001; Pilipenko *et al*., 2002; Surkov *et al*., 2005) have used a step-wise V_A profile, but it is more realistic to introduce a modified exponential profile, as suggested by Greifinger and Greifinger (1968) and used extensively in models of the IAR (e.g., Polyakov and Rapoport, 1981; Lysak, 1991, 1999; Trakhtengertz and Feldstein, 1991; Grzesiak, 2000; Pokhotelov *et al*., 2000) where

$$V_A^2(z) = \frac{V_{Ai}^2}{\epsilon^2 + e^{-z/h}}. \tag{21}$$

The wave structure is also determined by the ionospheric boundary condition, leading to a series of modes that are related to a characteristic frequency multiplied by zeroes of the zero-order Bessel function in the limit of high Pedersen conductance and to zeroes of the first-order Bessel function for low conductance (Lysak, 1991). In these cases the characteristic frequency scales with the ratio of the Alfvén velocity at the ionosphere divided by the ionospheric scale height, $V_{Ai}/2h$. For a typical Alfvén speed of 1000 km/s at the ionosphere and a scale height the order of 500 km, this characteristic angular frequency is 1.0 rad s^{-1} or a frequency of 0.16 Hz. Therefore, the fundamental eigenmode of the IAR is 0.38 to 0.61 Hz for the good conductivity and poor conductivity cases, respectively.

7. Simplified Model for the Fast Alfvén Mode in the IAR

While the density structure above the ionosphere leads to a resonance cavity for shear Alfvén waves, it provides a waveguide for fast mode waves that can propagate across field lines (e.g., Greifinger and Greifinger, 1968; Fraser, 1975). Therefore, a signal observed on the ground may not be on the same field line as the field-aligned current structure that produced it. Neudegg *et al*. (1995) have shown from an array of ground magnetometers that Pc1 signals propagate with a typical speed of 450 km/s over distances of a few hundred kilometers, consistent with propagation in this ionospheric waveguide. Yahnina *et al*. (2000) found that Pc1 oscillations can be seen a few hours of magnetic local time away from their source while Kim *et al*. (2011) showed examples of Pc1 events seen up to 3000 km from their source. These observations indicate that these waves can propagate over large distances through the ionosphere. Over such long distances, the magnetic field dip angle will change and so models that assume a vertical field require modification. The early work of Greifinger and Greifinger (1968, 1973) indicates that waves polarized in the poloidal or toroidal directions will interact with the ionosphere differently due to dip angle effects. Fujita and Tamao (1988) studied the propagation of Pc1 waves in a simplified model and also found changes in the polarization as the wave propagated.

A similar description as that surrounding Eq. (20) can be developed for the fast mode in the ionospheric waveguide. In this case waves can propagate horizontally in the waveguide and the wave equation takes the form

$$\frac{\partial E_y}{\partial z^2} + \left(\frac{\omega^2}{V_A^2(z)} - k_\perp^2 \right) E_y = 0. \tag{22}$$

The solution is obtained using the appropriate boundary conditions at the ionosphere. The difference here is that the fast mode propagates through to the ground and so the ground conductivity must be taken into account. The solutions in this case take the form of propagating modes that approach the eigenfrequencies of the shear mode resonator in the long-wavelength limit (Lysak, 2004; Lysak and Yoshikawa, 2006).

8. Effects of Hall Conductance on the IAR

The preceding discussion has considered the IAR for shear mode waves and the ionospheric waveguide for fast waves as separate entities, neglecting the effects of the Hall current. Hall conductance effects can be included in a similar way as discussed above for the lower frequency waves in relation to Eqs. (14)–(17). In order to show this mode coupling, take the divergence of Eq. (14), assuming the conductances are constant and the ambient magnetic field is vertical (Lysak and Song, 2006),

$$\begin{aligned} \nabla \cdot (\hat{\mathbf{z}} \times [\mathbf{b}]) &= -\hat{\mathbf{z}} \cdot (\nabla \times \mathbf{b}) = -j_z \\ &= \mu_0 (\Sigma_P \nabla \cdot \mathbf{E}_\perp - \Sigma_H \hat{\mathbf{z}} \cdot \nabla \times \mathbf{E}). \end{aligned} \tag{23}$$

We have assumed that there are no currents below the ionosphere. The condition in Eq. (14) also includes a condition on the fast mode magnetic field. This can be found by taking the vertical curl of Eq. (14) to give (Lysak and Song, 2006)

$$\left[\frac{\partial b_z}{\partial z} \right] = \mu_0 (\Sigma_P \hat{\mathbf{z}} \cdot \nabla \times \mathbf{E} + \Sigma_H \nabla \cdot \mathbf{E}_\perp). \tag{24}$$

While the jump in b_z is zero due to the divergence-free condition, the jump in its derivative can be non-zero. For vertical B_0, the shear mode is characterised by a non-zero divergence of $\mathbf{E}$ and the fast mode by a non-zero curl of $\mathbf{E}$. Therefore, Eqs. (23) and (24) show the role that the Hall conductance plays in coupling the two modes.

For oblique magnetic field dip angles, the degeneracy between the two perpendicular directions is broken, since

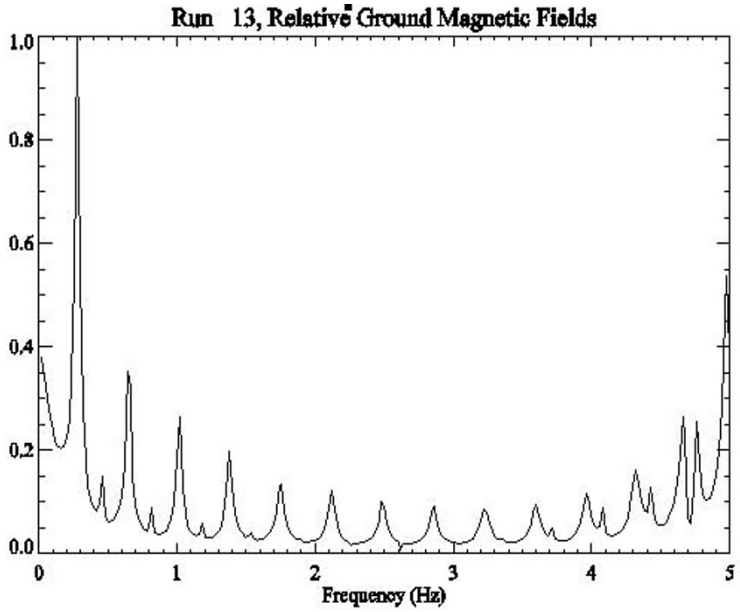

Fig. 6. Ground magnetic fields for waves trapped in the ionospheric Alfvén resonator. Parameters for the model run are given in the text.

waves with wave vectors in the latitudinal direction, in the plane of the dipole field, differ from those in the longitudinal direction. Sciffer and Waters (2002) and Sciffer *et al.* (2004) have analyzed the reflection and mode conversion of Alfvén and fast mode waves in the presence of oblique magnetic fields. They find a strong dependence on dip angle, especially for longitudinal propagation. One aspect of this interaction is that, while for vertical fields the magnetic fields due to field aligned and Pedersen currents cancel, this is no longer true for oblique fields. This is due in part to the presence of horizontal components of field aligned currents. Therefore, in the oblique magnetic field case the ground magnetic field can be non-zero even in the absence of Hall currents, as pointed out by Tamao (1986). Numerical modeling (Lysak, 2004) in a dipole model with oblique fields has confirmed that the coupling between the shear Alfvén modes and fast modes is present in this case.

The coupling between shear and fast modes in the IAR can be illustrated by observations of the spectral resonance structure of these modes. As an example, Hebden *et al.* (2005) observed harmonics up to almost 5 Hz from magnetometer data obtained from Sodankylä, Finland. These observations can be modeled using the equations in a tilted magnetic field geometry such as those introduced by Sciffer and Waters (2002). While this earlier work considered a uniform plasma density above the ionosphere, to study the IAR we can include a density profile of the form

$$n_e = n_0 e^{-z/h} + n_1 r^{-p} \tag{25}$$

where z is the altitude and r represents the geocentric distance along the flux tube. If we consider a wave with frequency ω and wave numbers k_x and k_y, Maxwell's equations can be written

$$\partial_z E_x = i\omega b_y - ik_x E_x \tan\alpha \tag{26}$$

$$\partial_z E_y = -i\omega b_x - ik_y E_x \tan\alpha \tag{27}$$

$$\partial_z b_x = -\frac{ik_x k_y}{\omega} E_x + \left(\frac{ik_x^2}{\omega} - \frac{i\omega}{V_A^2}\right) E_y \tag{28}$$

$$\partial_z b_y = \left(\frac{i\omega}{V_A^2 \cos^2\alpha} - \frac{ik_y^2}{\omega}\right) E_x + \frac{ik_x k_y}{\omega} E_y + i(k_y b_x - k_x b_y) \tan\alpha. \tag{29}$$

For Eqs. (26)–(29), the parallel electric field is set to zero and the z component of Faraday's Law is used to eliminate the b_z component. These equations are solved with an ionospheric boundary condition given by Eq. (14). The atmosphere is assumed to be a perfect insulator so that no currents flow there and the atmospheric magnetic field can be written as the gradient of a scalar potential that satisfies Laplace's equation, as discussed above.

Figure 6 shows the magnitude of the ground magnetic field, normalized to the incident Poynting flux, for a case where the tilt angle, α, is 16.1°. This corresponds to the conditions at Sodankylä, Finland. The spatial wave structure was $k_x = 10^{-3}$ km^{-1} and $k_y = 0$. The density profile was described by Eq. (25) with $n_0 = 10^5$ cm^{-3}, $n_1 = 1$ cm^{-3}, $h = 400$ km and $p = 0$. It is assumed that the exponential term in the electron density is balanced by oxygen ions, while the power law term is balanced by protons. The Pedersen and Hall conductances are each set to 10 S. These results show that multiple harmonics of the IAR can be excited in this situation, with frequencies consistent with those shown by Hebden *et al.* (2005).

9. Discussion

The importance of the ionospheric Hall conductance for ULF wave dynamics was recognised by Kato and Tamao (1956). Recent, renewed interest in the role of the anisotropic ionosphere and more detailed analyses using 1-D formulations for investigating ULF wave propagation properties have identified inductive feedback, oblique magnetic field and mode coupling effects. Our extension into

2-D models allows all these effects to be included for more realistic situations where parameters such as the field dip angle vary with latitude and the Alfvén speed varies in the magnetosphere.

The latitudinal spatial structure of field line resonances is poorly described by an $e^{i\mathbf{k}\cdot\mathbf{r}}$ model used in 1-D descriptions. The 2-D model in a meridian plane allows for self-consistent solutions that require a spectrum for $k_\perp$ in these structures in the Pc3–5 band. Simplified models have provided the essential ideas of energy balance when ionospheric Hall conductance effects are included. For example, the reduction in ionospheric Joule dissipation by the inductive Hall effect was examined by Yoshikawa (2002). Separation of the divergent and curl components of the ULF electric field into fast and shear Alfvén mode contributions are not possible for our varying magnetic field dip angle description. However, the essential ideas of energy exchange between an incident shear Alfvén wave (at resonance) and storage in the Hall current generated, fast mode are the same.

For the conditions in Fig. 3(a) with zero azimuthal spatial variation ($m = 0$), the decrease in Joule dissipation is clearly seen. At resonance locations, the reduced Joule heating coincides with an increase in the (evanescent) fast mode arising from the Hall conductance, inductive process. This occurs even for the Pc5 (5 mHz) wave frequency which demonstrates contributions to the inductive effect across resonance structures from the varying spatial scale.

Previous 1-D descriptions have studied the role of the ionospheric Hall conductance by initiating the process using an incident shear Alfvén description. Our 2-D model takes one step back in the sequence to excite the system with an inward propagating fast mode, which then couples with shear Alfvén modes in the magnetosphere for $m \neq 0$. Figure 3 shows the increased Joule dissipation at resonance locations seen in experimental data. However, the model results reveal details of the underlying processes. For a given inward propagating fast mode (e.g. 5 mHz), the first resonance mode coupling location (e.g. 8.5 R_E) shows up to 10% reduced Joule heating caused by the Hall conductance interaction. Energy is stored in the fast mode generated in the ionosphere due to the non-zero shear to fast mode conversion coefficient, cycling in time in a similar fashion to an inductor in an ac circuit. This interaction then affects the available energy to subsequent resonance locations further in the magnetosphere. One consequence is that Joule dissipation at a second resonance location (e.g. 6 R_E) may be increased, compared with the small Hall conductance case.

Most of the above work assumed a height-integrated conductivity in the ionosphere. This approximation is invalid for the Pc1 band. This is due to the finite collisional skin depth in the ionosphere, which becomes smaller than the ionospheric thickness at frequencies approaching 1 Hz. Lysak (1997, 1999) developed a model with a fully height resolved ionosphere to investigate the wave coupling under these conditions. This model illustrates the details of the rotation of the magnetic field as described above (Hughes, 1974) as well as the mode coupling between the fast and shear Alfvén modes. Sciffer *et al.* (2005) considered a resolved ionosphere and determined the reflection and mode coupling matrix for this system. These studies show that while the details of the reflection and mode coupling depend on the structure of the ionosphere, the basic features seen in the height-integrated model of the ionosphere are preserved.

New theoretical developments beyond those presented above have concentrated on the interaction of the resonator with parallel electric fields and the acceleration of auroral particles. Lysak (1993) included electron inertia and a more realistic V_A profile based on a dipole magnetic field to show that effects from the resonator persisted when parallel electric fields were present. This model was used to investigate electron acceleration through test particle models (Thompson and Lysak, 1996; Chaston *et al.*, 2000, 2002a), indicating that field aligned beams of electrons observed from the FAST satellite were consistent with acceleration due to parallel electric fields in the resonator.

The role of parallel electric fields in strengthening the reflection of Alfvén waves near the V_A peak has been emphasized by Pilipenko *et al.* (2002, 2004). Although these authors considered the reflection from the parallel electric field region as defining a different resonator, the same low densities that produce the Alfvén speed peak also favor the formation of parallel electric fields. Therefore, it seems that parallel electric fields modify the ionospheric Alfvén resonator rather than represent a new resonator.

There are other potential applications in modeling these waveguide and cavity structures. In the auroral zone, the excitation of waves in the ionospheric Alfvén resonator can lead to the acceleration of auroral electrons (e.g., Chaston *et al.*, 2002a, b; Chaston, 2006). These waves can also play a role in conductivity variations in the auroral zone leading to a feedback instability (e.g., Lysak, 1991; Lysak and Song, 2002; Pokhotelov *et al.*, 2002), which may be a critical ingredient in the formation of narrow auroral arcs (e.g., Newell *et al.*, 1996).

10. Conclusion

The coupling of magnetospheric ULF waves through the ionosphere, atmosphere and to the ground allows for the observation of these waves by ground magnetometers, even at lower frequencies where the atmospheric modes may be evanescent. The importance of the ionospheric Hall conductivity has been recently revived and described using one dimensional models.

We have presented results from a 2-D, time dependent model that includes ionospheric Hall current effects and uses a dipole geometry. For the lower ULF frequencies that form FLRs in the magnetosphere the Hall conductance reduces the Joule heating in the ionosphere, effectively increasing the reactive component of the resonant system, which appears as evanescent fast mode signals. We are presently developing 3-D descriptions that will allow quantification of energy that propagates azimuthally from these resonance regions.

At Pc1 frequencies, the fast mode signal can propagate in the ionospheric waveguide and be seen over 1000 km from their source. These waves can be excited by magnetospheric-imposed field aligned currents carried by the shear Alfvén wave, followed by mode conversion due to

the Hall conductivity of the ionosphere. Simultaneous observations of Pc1 and Pi1 signals both in space and on the ground (Arnoldy *et al.*, 1996, 1998; Lessard *et al.*, 2006) confirm this link between magnetospheric and atmospheric fields. Therefore, the existence of these waveguide modes, in addition to the coupling caused by the anisotropic conductivity in the ionosphere is essential for understanding ground magnetometer data and its use to understand the field aligned currents entering the ionosphere.

Acknowledgments. This research was supported by NSF grant NSF/ATM-1015310 for the work in Minnesota and an ARC-DP grant from the Australian Research Council for the work in Newcastle.

References

Alfvén, H. and C.-G. Fälthammar, *Cosmical Electrodynamics*, Oxford Univ. Press, 1963.

Alperovich, L. S. and E. N. Fedorov, On hydromagnetic wave beams propagation through the ionosphere, *Ann. Geophys.*, **10**, 647, 1992.

Anderson, B. J. and M. J. Engebretson, Distortion effects in spacecraft observations of MHD toroidal standing waves, Theory and observations, *J. Geophys. Res.*, **94**(A10), 13425–13445, 1989.

Arnoldy, R. L., M. J. Engebretson, and L. J. Cahill, Bursts of Pc1-2 near the ionospheric footprint of the cusp and their relationship to flux transfer events, *J. Geophys. Res.*, **93**, 1007, 1988.

Arnoldy, R. L., M. J. Engebretson, J. L. Alford, R. E. Erlandson, and B. J. Anderson, Magnetic impulse events and associated Pc1 bursts at dayside high latitudes, *J. Geophys. Res.*, **101**, 7793, 1996.

Arnoldy, R. L., J. L. Posch, M. J. Engebretson, H. Fukunishi, and H. J. Singer, Pi1 magnetic pulsations in space and at high latitudes on the ground, *J. Geophys. Res.*, **103**, 23,581, 1998.

Ashour, A. A. and A. T. Price, The induction of electric current in a nonuniform ionosphere, *Proc. R. Soc. Lond., A*, **195**, 198–224, 1948.

Belyaev, P. P., T. Bösinger, S. V. Isaev, and J. Kangas, First evidence at high latitudes for the ionospheric Alfvén resonator, *J. Geophys. Res.*, **104**, 4305, 1999.

Berthelier, A., J.-C. Cerisier, J.-J. Berthelier, J.-M. Bosqued, and R. A. Kovrazkhin, The electrodynamic signature of short scale field aligned currents, and associated turbulence in the cusp and dayside auroral zone, in *Electromagnetic Coupling in the Polar Clefts and Caps*, edited by P. E. Sandholt and A. Egeland, p. 299, Kluwer, Dordrecht, 1989.

Block, L. P. and C.-G. Fälthammar, The role of magnetic-field-aligned electric fields in auroral acceleration, *J. Geophys. Res.*, **95**, 5877, 1990.

Boehm, M. H., C. W. Carlson, J. P. McFadden, J. H. Clemmons, and F. S. Mozer, High-resolution sounding rocket observations of large amplitude Alfvén waves, *J. Geophys. Res.*, **95**, 12,157, 1990.

Chaston, C. C., ULF waves and auroral electrons, in *Magnetospheric ULF Waves*, edited by K. Takahashi *et al.*, AGU Monograph Series, p. 289, AGU, Washington, 2006.

Chaston, C. C., C. W. Carlson, R. E. Ergun, and J. P. McFadden, Alfvén waves, density cavities and electron acceleration observed from the FAST spacecraft, *Physica Scripta*, **T84**, 64–68, 2000.

Chaston, C. C., J. W. Bonnell, L. M. Peticolas, C. W. Carlson, J. P. McFadden, and R. E. Ergun, Driven Alfvén waves and electron acceleration: A FAST case study, *Geophys. Res. Lett.*, **29**(11), doi:10.1029/2001GL013842, 2002a.

Chaston, C. C., J. W. Bonnell, C. W. Carlson, M. Berthomier, L. M. Peticolas, I. Roth, J. P. McFadden, R. E. Ergun, and R. J. Strangeway, Electron acceleration in the ionospheric Alfvén resonator, *J. Geophys. Res.*, **107**(A11), 1413, doi:10.1029/2002JA009272, 2002b.

Chmyrev, V. M., V. N. Oraevsky, S. V. Bilichenko, N. V. Isaev, G. A. Stanev, D. K. Teodosiev, and S. I. Shkolnikova, The fine structure of intensive small scale electric and magnetic fields in the high latitude ionosphere as observed by Inter-cosmos-Bulgaria-1300 satellite, *Planet. Space Sci.*, **33**, 1383, 1985.

D'haeseleer, W. D., W. N. G. Hitchon, J. D. Callen, and J. L. Shohet, *Flux Coordinates and Magnetic Field Structure*, Springer-Verlag, New York, 1991.

Dungey, J. W., Hydromagnetic waves and the ionosphere, *Proc. Int. Conf. Ionos., Rep.*, **230**, Inst. of Phys., London, 1963.

Erlandson, R. E., L. J. Zanetti, T. A. Potemra, L. P. Block, and G. Holmgren, Viking magnetic and electric field observations of Pc1 waves at high latitudes, *J. Geophys. Res.*, **95**, 5941, 1990.

Fedorov, E., V. Pilipenko, and M. J. Engebretson, ULF wave damping in the auroral acceleration region, *J. Geophys. Res.*, **106**(A4), 6203–6212, 2001.

Francis, W. E. and R. Karplus, Hydromagnetic waves in the ionosphere, *J. Geophys. Res.*, **65**, 3593–3600, 1960.

Fraser, B. J., Ionospheric duct propagation and Pc1 pulsation source, *J. Geophys. Res.*, **80**, 2790, 1975.

Fujita, S. and T. Tamao, Duct propagation of hydromagnetic waves in the upper ionosphere, 1, Electromagnetic field disturbances in high latitudes associated with localized incidence of a shear Alfvén wave, *J. Geophys. Res.*, **93**, 14,665, 1988.

Greenwald, R. A. and A. D. M. Walker, Energetics of long period resonant hydromagnetic waves, *Geophys. Res. Lett.*, **7**, 745, 1980.

Greifinger, C. and P. Greifinger, Theory of hydromagnetic propagation in the ionospheric waveguide, *J. Geophys. Res.*, **73**, 7473, 1968.

Greifinger, C. and P. Greifinger, Wave guide propagation of micropulsations out of the plane of the geomagnetic meridian, *J. Geophys. Res.*, **78**, 4611, 1973.

Grzesiak, M., Ionospheric Alfvén resonator as seen by Freja satellite, *Geophys. Res. Lett.*, **27**, 923, 2000.

Gurnett, D. A., R. L. Huff, J. D. Menietti, J. L. Burch, J. D. Winningham, and S. D. Shawhan, Correlated low-frequency electric and magnetic noise along auroral field lines, *J. Geophys. Res.*, **89**, 8971, 1984.

Hansen, H. D., B. J. Fraser, F. W. Menk, Y.-D. Hu, P. T. Newell, C.-I. Meng, and R. J. Morris, High-latitude Pc1 bursts arising in the dayside boundary layer region, *J. Geophys. Res.*, **97**, 3993, 1992.

Hebden, S. R., T. R. Robinson, D. M. Wright, T. Yeoman, T. Raita, and T. Bösinger, A quantitative analysis of the diurnal evolution of Ionospheric Alfvén resonator magnetic resonance features and calculation of changing IAR parameters, *Ann. Geophys.*, **23**, 1711–1721, 2005.

Hirano, Y., H. Fukunishi, R. Kataoka, T. Hasunuma, T. Nagatsuma, W. Miyake, and A. Matsuoka, Evidence for the resonator of inertial Alfvén waves in the cusp topside ionosphere, *J. Geophys. Res.*, **110**, A07218, doi:10.1029/2003JA010329, 2005.

Hughes, W. J., The effect of the atmosphere and ionosphere on long period magnetospheric micropulsations, *Planet. Space Sci.*, **22**, 1157, 1974.

Iyemori, T. and K. Hayashi, Pc1 micropulsations observed by Magsat in the ionospheric F region, *J. Geophys. Res.*, **94**, 93, 1989.

Jackson, J. D., *Classical Electrodynamics*, John Wiley and Sons, Inc., New York, 1999.

Jacobs, J. A. and T. Watanabe, Propagation of hydromagnetic waves in the lower exosphere and the origin of short period geomagnetic pulsations, *J. Atmos. Terr. Phys.*, **24**, 413, 1962.

Jacobs, J. A., Y. Kato, S. Matsushita, and V. A. Troitskaya, Classification of geomagnetic micropulsations, *J. Geophys. Res.*, **69**, 180, 1964.

Kato, Y. and T. Tamao, Hydromagnetic oscillations in a conducting medium with Hall conductivity under the uniform magnetic field, *Sci. Rept. Tohoku Univ. Ser. 5, Geophys.*, **7**(3), 147, 1956.

Kim, H., M. R. Lessard, M. J. Engebretson, and M. A. Young, Statistical study of Pc 1-2 wave propagation characteristics in the high-latitude ionospheric waveguide, *J. Geophys. Res.*, **116**, A077227, doi:10.1029/2010JA016355, 2011.

Knudsen, D. J., M. C. Kelley, G. D. Earle, J. F. Vickrey, and M. Boehm, Distinguishing Alfvén waves from quasi-static field structures associated with discrete aurora: Sounding rocket and HILAT measurements, *Geophys. Res. Lett.*, **17**, 921, 1990.

Knudsen, D. J., M. C. Kelley, and J. F. Vickrey, Alfvén waves in the auroral ionosphere: a numerical model compared with measurements, *J. Geophys. Res.*, **97**, 77, 1992.

Lessard, M. R., E. J. Lund, S. L. Jones, R. L. Arnoldy, J. L. Posch, M. J. Engebretson, and K. Hayashi, Nature of Pi1B pulsations as inferred from ground and satellite observations, *Geophys. Res. Lett.*, **33**, L14108, doi:10.1029/2006GL026411, 2006.

Lysak, R. L., Coupling of the dynamic ionosphere to auroral flux tubes, *J. Geophys. Res.*, **91**, 7047, 1986.

Lysak, R. L., Feedback instability of the ionospheric resonant cavity, *J. Geophys. Res.*, **96**, 1553, 1991.

Lysak, R. L., Generalized model of the ionospheric Alfvén resonator, in *Auroral Plasma Dynamics*, edited by R. L. Lysak, AGU Monograph 80, p. 121, 1993.

Lysak, R. L., Propagation of Alfvén waves through the ionosphere, *Phys. Chem. Earth*, **22**, 757, 1997.

Lysak, R. L., Propagation of Alfvén waves through the ionosphere: Dependence on ionospheric parameters, *J. Geophys. Res.*, **104**, 10,017, 1999.

Lysak, R. L., Magnetosphere-ionosphere coupling by Alfvén waves at mid-latitudes, *J. Geophys. Res.*, **109**, A07201, doi:10.1029/2004JA010454, 2004.

Lysak, R. L. and Y. Song, Energetics of the ionospheric feedback interaction, *J. Geophys. Res.*, **107**(A8), doi:10.1029/2001JA000308, 2002.

Lysak, R. L. and Y. Song, Magnetosphere-ionosphere coupling by Alfvén waves: Beyond current continuity, *Adv. Space Res.*, **38**(8), 1713, 2006.

Lysak, R. L. and A. Yoshikawa, Resonant cavities and waveguides in the ionosphere and atmosphere, in *Magnetospheric ULF Waves*, edited by K. Takahashi *et al.*, AGU Monograph Series, p. 289, AGU, Washington, 2006.

Manchester, R. N., Correlation of Pc1 micropulsations at spaced stations, *J. Geophys. Res.*, **73**, 3549, 1968.

Marklund, G. T., L. G. Blomberg, C.-G. Fälthammar, R. E. Erlandson, and T. A. Potemra, Signatures of the high-altitude polar cusp and dayside aurora regions as seen by the Viking electric field experiment, *J. Geophys. Res.*, **95**, 5767, 1990.

Neudegg, D. A., B. J. Fraser, F. W. Menk, H. J. Hansen, G. B. Burns, R. J. Morris, and M. J. Underwood, Source and velocities of Pc1-2 ULF waves at high latitudes, *Geophys. Res. Lett.*, **22**, 2965, 1995.

Newell, P. T., C.-I. Meng, and K. M. Lyons, Suppression of discrete aurora by sunlight, *Nature*, **381**, 766, 1996.

Nishida, A., Ionospheric screening effect and storm sudden commencement, *J. Geophys. Res.*, **69**, 1861, 1964.

Obana, Y., A. Yoshikawa, J. V. Olson, R. J. Morris, B. J. Fraser, and K. Yumoto, North-south asymmetry of the amplitude of high-latitude Pc 3–5 pulsations: Observations at conjugate stations, *J. Geophys. Res.*, **110**, A10214, doi:10.1029/2003JA010242, 2005.

Olson, J. V. and G. Rostoker, Longitudional phase variation of Pc 4–5 micropulsations, *J. Geophys. Res.*, **83**(A6), 2481–2488, 1978.

Pilipenko, V. A., M. Vellante, and E. N. Fedorov, Distortion of the ULF wave spatial structure upon transmission through the ionosphere, *J. Geophys. Res.*, **105**(A9), 21,225–21,236, doi:10.1029/2000JA900063, 2000.

Pilipenko, V. A., E. N. Fedorov, and M. J. Engebretson, Alfvén resonator in the topside ionosphere beneath the auroral acceleration region, *J. Geophys. Res.*, **107**(A9), 1257, doi:10.1029/2002JA009282, 2002.

Pilipenko, V., E. Fedorov, M. J. Engebretson, and K. Yumoto, Energy budget of Alfvén wave interactions with the auroral acceleration region, *J. Geophys. Res.*, **109**, A10204, doi:10.1029/2004JA010440, 2004.

Polyakov, S. V. and V. O. Rapoport, Ionospheric Alfvén resonator, *Geomag. Aeron.*, **21**, 816, 1981.

Pokhotelov, D., W. Lotko, and A. V. Streltsov, Harmonic structure of field line eigenmodes generated by ionospheric feedback instability, *J. Geophys. Res.*, **107**(A11), 1363, doi:10.1029/2001JA000134, 2002.

Pokhotelov, O., D. Pokhotelov, A. Streltsov, V. Khruschev, and M. Parrot, Dispersive ionospheric Alfvén resonator, *J. Geophys. Res.*, **105**, 7737, 2000.

Popecki, M., R. Arnoldy, M. J. Engebretson, and L. J. Cahill, High-latitude ground observations of Pc1/2 micropulsations, *J. Geophys. Res.*, **98**, 21,481, 1993.

Potemra, T. A., R. E. Erlandson, L. J. Zanetti, R. L. Arnoldy, J. Woch, and E. Friis-Christensen, The dynamic cusp, *J. Geophys. Res.*, **97**, 2835, 1992.

Scholer, M., On the motion of artificial ion clouds in the magnetosphere, *Planet. Space Sci.*, **18**, 977, 1970.

Sciffer, M. D. and C. L. Waters, Propagation of ULF waves through the ionosphere: Analytic solutions for oblique magnetic fields, *J. Geophys. Res.*, **107**(A10), 1297, doi:10.1029/2001JA000184, 2002.

Sciffer, M. D., C. L. Waters, and F. W. Menk, Propagation of ULF waves through the ionosphere: Inductive effect for oblique magnetic fields, *Ann. Geophys.*, **22**, 1155, 2004.

Sciffer, M. D., C. L. Waters, and F. W. Menk, A numerical model to investigate the polarization azimuth of ULF waves through an ionosphere with oblique magnetic fields, *Ann. Geophys.*, **23**, 3457, 2005.

Sorokin, V. M., The role of the ionosphere in the propagation of geomagnetic pulsations, *Geomagn. Aeron.*, **26**, 532, 1986.

Stix, T. H., *The Theory of Plasma Waves*, McGraw-Hill, New York, 1962.

Surkov, V. V., O. A. Molchanov, M. Hayakawa, and E. N. Fedorov, Excitation of the ionospheric resonance cavity by thunderstorms, *J. Geophys. Res.*, **110**, A04308, doi:10.1029/2004JA010850, 2005.

Taflove, A. and S. C. Hagness, *Computational Electrodynamics: The Finite-Difference Time-Domain Method*, Artech House Inc., 2005.

Tamao, T., Transmission and coupling resonance of hydromagnetic disturbances in the non-uniform Earth's magnetosphere, *Sci. Rept. Tohoku Univ. Ser. 5, Geophys.*, **17**(2), 43, 1965.

Tamao, T., Direct contribution of oblique field-aligned currents to ground magnetic fields, *J. Geophys. Res.*, **91**(A1), 183–189, doi:10.1029/JA091iA01p00183, 1986.

Tanaka, H., Y. Saito, K. Asamura, S. Ishii, and T. Mukai, High time resolution measurement of multiple electron precipitations with energy-time dispersion in high-latitude part of the cusp region, *J. Geophys. Res.*, **110**, A07204, doi:10.1029/2004JA010664, 2005.

Temerin, M., C. Cattell, R. Lysak, M. Hudson, R. B. Torbert, F. S. Mozer, R. D. Sharp, and P. M. Kintner, The small scale structure of electrostatic shocks, *J. Geophys. Res.*, **86**, 11,278, 1981.

Thompson, B. J. and R. L. Lysak, Electron acceleration by inertial Alfvén waves, *J. Geophys. Res.*, **101**, 5359, 1996.

Trakhtengertz, V. Yu. and A. Ya. Feldstein, Quiet auroral arcs: Ionospheric effect of magnetospheric convection stratification, *Planet. Space Sci.*, **32**, 127, 1984.

Trakhtengertz, V. Yu. and A. Ya. Feldstein, Turbulent Alfvén boundary layer in the polar ionosphere, I, Excitation conditions and energetics, *J. Geophys. Res.*, **96**, 19,363, 1991.

Volwerk, M., P. Louarn, T. Chust, A. Roux, and H. de Feraudy, Solitary kinetic Alfvén waves: A study of the Poynting flux, *J. Geophys. Res.*, **101**, 13,335, 1996.

Waters, C. L. and M. D. Sciffer, Field line resonant frequencies and ionospheric conductance: Results from a 2-D MHD model, *J. Geophys. Res.*, **113**, A05219, doi:10.1029/2007JA012822, 2008.

Yahnina, T. A., A. G. Yahnin, J. Kangas, and J. Manninen, Proton precipitation related to Pc1 pulsations, *Geophys. Res. Lett.*, **27**, 3575, 2000.

Yoshikawa, A., Excitation of a Hall-current generator by field-aligned current closure, via an ionospheric, divergent Hall-current, during the transient phase of magnetosphere-ionosphere coupling, *J. Geophys. Res.*, **107**, 1445, doi:10.1029/2001JA009170, 2002.

Yoshikawa, A. and M. Itonaga, Reflection of shear Alfvén waves at the inductive ionosphere, *Geophys. Res. Lett.*, **23**, 101, 1996.

Yoshikawa, A. and M. Itonaga, The nature of reflection and mode conversion of MHD waves in the inductive ionosphere: Multistep mode conversion between divergent and rotational electric fields, *J. Geophys. Res.*, **105**, 10,565, 2000.

Yoshikawa, A., Y. Obana, M. Shinohara, M. Itonaga, and K. Yumoto, Hall-induced inductive shielding effect on geomagnetic pulsations, *Geophys. Res. Lett.*, **29**(8), 1266, doi:10.1029/2001GL013610, 2002.

C. L. Waters (e-mail: colin.waters@newcastle.edu.au), R. L. Lysak, and M. D. Sciffer